Interrogation of Vibrational Structure and Line Broadening of Liquid Water by Raman-Induced Kerr Effect Measurements within the Multimode Brownian Oscillator Model†

Stephen Palese,‡ Shaul Mukamel, and R. J. Dwayne Miller*,§

Department of Chemistry, University of Rochester, Rochester, New York 14627

William T. Lotshaw*

General Electric Research and Development Center, P.O. Box 8, Room KWC-627, Schenectady, New York 12301

Received: January 26, 1996; In Final Form: April 1, 1996⊗

The method used to deduce the spectral density distribution of intermolecular and intramolecular (vibrational) degrees of freedom in the liquid state from optical heterodyne detected optical (Raman-induced) Kerr effect (OHD-RIKE) measurements is reexamined within a multimode Brownian oscillator model. The ramifications of nonlinear coupling of the nuclear degrees of freedom to the medium polarizability are explored for discrimination between "homogeneous" and "inhomogeneous" contributions to the vibrational spectral density. Under physically reasonable assumptions, an estimation of the homogeneous contribution to the vibrational line shape can be made from the OHD-RIKE observable (if nonlinear coupling is nonnegligible). The model is developed generally, and calculations are applied specifically to temperature-dependent OHD-RIKE measurements of liquid water. The results indicate that the line broadening in the low-frequency vibrational distribution due to the hydrogen-bonded network structure of liquid water is mostly inhomogeneous, with an effective homogeneous relaxation time of 350 fs at 24 °C.

Introduction

The nature of the motions and relaxation processes of intermolecular degrees of freedom in molecular liquids has important ramifications for chemical processes in solution. Of particular interest is the time scale for irreversible reorganization of solvent structure around excited solute species, which can affect the outcome of chemical reactions where dynamics along a "solvation coordinate" are rate-limiting. Extensive spectroscopic investigations of these dynamics have been conducted using for example spontaneous Raman and femtosecond optical Kerr techniques. Due to the complexity of molecular liquids, the motions and relaxations span a broad range of time scales (static to femtosecond). The low-frequency motions $<800\ \mathrm{cm}^{-1}$ contain information about the structure and dynamics of collective intermolecular interactions and can be probed by ultrafast coherent Raman spectroscopies.[1−6]

A major complication in a modal analysis of the spectral density function of these degrees of freedom is that a static distribution of environments usually makes a significant contribution to the line widths of the individual modes. The dominance of this effect makes an interrogation of the dynamical contribution to the line widths difficult. Ideally, one would like to make a clear distinction between the "fast" and "slow" contributions to the linewidths. Static (or very slow) contributions are conventionally denoted "inhomogeneous broadening" as opposed to the "homogeneous" fast contributions, which give rise to the more interesting and relevant structural dynamics of the medium. Such distinctions are possible only when a clear separation of time scales distinguishes these contributions. When the system is characterized by a continuous distribution of time scales (as in the case of molecular liquids), it is advantageous to describe the system degrees of freedom with a continuous spectral density function, and the distinction between "homogeneous" and "inhomogeneous" contributions may not be possible. Operationally, one can define the spontaneous Raman signal or the Fourier transform of the Raman-induced Kerr effect (RIKES) signal as the spectral density of the system degrees of freedom. However, this definition does not provide insight into the microscopic interpretation of the spectra. Therefore, despite the difficulties outlined above, it is tempting to retain the notions of homogeneous and inhomogeneous processes. This is theoretically possible by decomposing the spectral density into a homogeneous part $J(\omega;\Gamma)$ that depends on coupling parameters and dynamical constants Γ and an inhomogeneous distribution of these parameters $S(\Gamma)$. The experimental spectral density is then given by the convolution of these quantities

$$C(\omega) = \int J(\omega;\Gamma)\, S(\Gamma)\, \mathrm{d}\Gamma \tag{1}$$

A simple measurement of $C(\omega)$ as produced by the spontaneous Raman or femtosecond RIKES techniques cannot directly reveal the contributions J and S separately, and there are many possible choices of J and S giving the same $C(\omega)$ which may be unphysical or not objectively distinguishable. Nevertheless, this decomposition of $C(\omega)$ makes sense if J and S can be independently manipulated and measured. It has been shown that higher-order Raman measurements, which involve more than one time evolution period, constitute a multidimensional spectroscopy which can directly distinguish the homogeneous and inhomogeneous contributions.[7] Such experiments are technically very demanding and currently in progress. In this paper, we propose a different procedure. We show that a series of RIKES measurements, where the temperature (or possibly

† Presented at the Northeast Regional ACS Meeting in Rochester, NY (October 24 and 25, 1995), on the "Structure and Dynamics of Liquids".

‡ Current address: Department of Chemistry, University of Pennsylvania, Philadelphia, PA 19020.

§ Current address: Department of Chemistry, 80 St. George Street, University of Toronto, Toronto, Ontario, Canada M5S1A1.

* Corresponding authors.

⊗ Abstract published in *Advance ACS Abstracts,* May 15, 1996.

S0022-3654(96)00266-3 CCC: $12.00

another state parameter) is varied, can be used to distinguish the contributions of *J* and *S* to the third-order RIKES response function. This analytical procedure depends on a specific model of the nonlinear optical response of the medium, unlike the higher-order techniques which are model independent. Our analysis is based on the nonlinear dependence of the medium polarizability on the intramolecular and intermolecular degrees of freedom (coordinates). The nature of the coupling of the coordinates to the polarizability has important ramifications for the connection of molecular dynamics and normal mode simulations to experimental measurements of the Raman spectral density.

Theory

Fourier-transform analysis of the femtosecond time-resolved optical heterodyne detected Raman-induced Kerr effect (OHD-RIKE) transient wave form directly recovers[8] the spectral density distribution $C(\omega)$ underlying the third-order susceptibility ($\chi^{(3)}$) under certain assumptions. Of these, the principal one is that the medium polarizability is a linear function of the intramolecular and intermolecular nuclear coordinates. Then the line broadening mechanisms for these degrees of freedom contribute to the spectral density function $C(\omega)$, and the response function $R^{(3)}(\tau)$ (*vide infra*) in the same way, and no objective basis exists for an evaluation of the time ordering or coupling between them. On this basis, information about line broadening of the spectroscopic transitions associated with these coordinates is inaccessible to the OHD-RIKE measurement taken at a single set of state parameters. When the medium polarizability depends nonlinearly on the nuclear coordinates, the nonlinear optical response of the medium acquires contributions which may be distinguishable by their functional dependencies on state variables such as temperature, isotopic composition, and chemical composition. The distinctions derive from differing functional dependencies of the *J* and *S* contributions to the spectral density $C(\omega)$ on these variables and can be quantified by theoretical nonlinear optical response functions derived from the multimode Brownian oscillator model[7] for the intermolecular degrees of freedom fitted to the measured OHD-RIKE transients. In this way, it is possible to distinguish homogeneous and inhomogeneous contributions to bands in the vibrational spectral density function by a series of third-order nonlinear optical measurements.

The semiclassical Brownian oscillator model of Tanimura and Mukamel[7a] treats the molecular and intermolecular coordinates as a distribution of harmonic oscillators. (The generalization to nonharmonic oscillators is in progress.) In general, the dependence of the polarizability $\alpha(Q)$ on the (set of) nuclear degrees of freedom (modes) Q can be represented by a polynomial series:

$$\alpha(Q) = \sum_{n=1}^{\infty} \frac{1}{n!} \alpha_n Q^n \tag{2}$$

where the coefficients α_n are given by the differential $(\partial^n\alpha/\partial Q^n)$ of the polarizability α in a finite volume of the medium. The coordinate dependence in eq 2 has been described previously by an exponential generating function $\alpha(Q) = \alpha_0 \exp(\sum_s A_s Q_s)$ for simplicity and generality.[7] The polynomial form can be derived from the exponential generating function and was chosen here since the expansion is taken only to the quadratic term in the present example (*vide infra*). For $n > 1$ in eq 2, the α_n can be regarded as identifying contributions to the bulk polarizability due to nonlinear coupling of n nuclear degrees of freedom in the polarizability of the medium. Note that the degrees of freedom Q in eq 2 are not (necessarily) the configurational and structural coordinates of molecules and their nearest neighbors found in the pairwise multipole expansion of the molecular polarizability. Equation 2 describes the coupling of structural coordinates which emerge from a vibrational mode analysis of the local molecular configuration under the influence of intermolecular forces due to contributions to the intermolecular potential such as the multipole expansion.[9] The linear approximation decomposes the medium polarizability into a basis set of modal contributions Q, some of which are molecular and some of which are intermolecular, arising from interactions like those described by the multipole potential The nonlinear hypothesis considers the static and dynamic coupling between individual modes in this set of (basis) coordinates Q. Such a representation can be regarded as an extrapolation of the theory for "interaction-induced" contributions to the Raman susceptibility developed by Madden *et al.*,[10] where the identification of (i) the modes Q and (ii) the coupling between them (*e.g.*, eq 2) arise from terms in the intermolecular potential that are linear and higher order in the Q, respectively.

The nonlinear response functions have been derived within both path-integral[7a] and quantum mechanical coherent state[7b] formalisms. While the results presented below are the same in either formalism, the traditional sum-over-states interpretation of optical response functions in terms of populations and coherences between specific levels is more transparent in the latter derivation. The third-order optical response can be written to second order in the coordinates Q as

$$R^{(3)}(\tau) = \frac{2i\alpha_1^{\,2}}{\hbar} \int d\Gamma\, S(\Gamma)\, C''(\tau,\Gamma) + \frac{2i\alpha_2^{\,2}}{\hbar} \int d\Gamma\, S(\Gamma)\, C''(\tau,\Gamma)\, C'(\tau,\Gamma) \tag{3}$$

where

$$C''(\tau) = \int d\omega\, J(\omega;\Gamma) \sin \omega\tau \tag{4}$$

$$C'(\tau) = \int d\omega'\, J(\omega';\Gamma) \cos \omega'\tau \coth \frac{\beta\hbar\omega'}{2} \tag{5}$$

are the imaginary and real parts of the correlation function for the nuclear degrees of freedom (modes) Q. $S(\Gamma)$ is the inhomogeneous distribution of oscillators and $J(\omega;\Gamma)$ is the homogeneous spectral density for each given realization of $S(\Gamma)$, where $\beta = 1/kT$ (k is the Boltzmann constant and T the temperature). Γ represents the distribution of parameters for each oscillator (η_s, γ_s, ω_s) where η_s is the coupling strength, γ_s is the damping, and ω_s is the center frequency for each mode.

When the polarizability is linear in the coordinates Q, $\alpha(Q) = \alpha_1 Q_1$ and only the lowest-order term (with the coefficient α_1^2) of $R^{(3)}(\tau)$ is nonzero, with all higher-order responses ($R^{(5)}$, $R^{(7)}$, ⋯) identically zero.[7] In this case the set of nuclear coordinates Q specify noninteracting "normal modes" of the medium structure, giving

$$R^{(3)}(\tau) \propto \int d\Gamma\, S(\Gamma) \int d\omega\, J(\omega;\Gamma) \sin \omega\tau \tag{6}$$

The discrete Fourier-transform (DFT) technique introduced by Lotshaw *et al.*[8a] and extensively developed by McMorrow, Lotshaw, and co-workers[6,8b,9] extracts the spectral density distribution $C(\omega)$, which can also be recovered by spontaneous light scattering (after significant data manipulation) and stimu-

lated Raman gain measurements. While there are many attributes which recommend the OHD-RIKE method for the purpose of obtaining $C(\omega)$,[9] neither the spectral line broadening contributions $S(\Gamma)$ and $J(\omega;\Gamma)$ to $C(\omega)$ nor mode couplings can be directly evaluated since all degrees of freedom, including bath interactions, contribute to $R^{(3)}(\tau)$ through $S(\Gamma)$ and $J(\omega;\Gamma)$ in the same way.

The major problem with the linear polarizability hypothesis is the difficulty of eq 6 to account for measured parametric dependencies in the long-lived exponential relaxations which have been observed in the OHD-RIKE response of hydrogen-bonded, network-forming liquids like water.[6] In molecular liquids exhibiting less structure and less specific interactions, these contributions have been attributed to reorientational diffusion processes[2,8] and therefore fit to classical rotational Brownian models (*i.e.*, Debye−Stokes−Einstein (DSE) model). The previously noted excellent agreement between the longest-lived exponential relaxation observed in the femtosecond OHD-RIKE, dynamic light scattering (DLS), and NMR measurements of molecular orientational dynamics in "simple" organic liquids supported this attribution.[2,8] Such agreement, however, is lacking with the reorientation rate of water molecules deduced from dielectric relaxation and NMR studies,[11] which is over an order of magnitude slower than the slowest exponential relaxation observed in the femtosecond OHD-RIKE transient[6] (*i.e.*, $\tau_{1/e} = 8$ ps for NMR, dielectric relaxation; 0.6 ps for OHD-RIKES[12] at 24 °C). In part, it is the lack of convergence between the lifetimes derived from these diverse measurements which suggests that the quasi-exponential behavior of the RIKES transient of water at times longer than 1 ps may partly arise from nonlinear coupling of the nuclear coordinates (Q) to the bulk (optical) polarizability.

The DSE contributions to the OHD-RIKE response have been previously approximated by a data reduction ("tail-matching") procedure[8] in which an overdamped oscillator response function with the same decay rate and amplitude as the presumed DSE contribution is subtracted from the OHD-RIKE transient in order to generate a purely "vibrational" spectral density from the DFT operation.[8] This procedure makes assumptions regarding the rise time of the oscillator response (through the moment of inertia of the oscillator and the resistance of the medium) and therefore may distort the spectral density distribution determined by the DFT analysis of the reduced data. Furthermore, unless the polarizability is strictly linear in the medium coordinates Q, the subtraction of a single response component from the set of coupled components in $R^{(3)}(\tau)$ is theoretically inconsistent with eq 3, in which the same dynamical coordinate (as an element of Q) can contribute to more than one of the integral terms of the response $R^{(3)}(\tau)$. In order to justify the component subtraction, two conditions must be satisfied: first, the coupling of the polarizability and nuclear coordinates must be strictly linear; second, the intermolecular modes must be divided into at least two groups, with a band at the lowest frequencies leading to diffusive motions. Such a division was proposed by Ohmine and Tanaka,[13] subsequently discussed by Cho *et al.*,[14] and implied by the "tail-matching" procedure of McMorrow and Lotshaw[8] described above. Due to the conditions enumerated above, pure linear coupling of the polarizability to the nuclear degrees of freedom Q explicitly means that higher-order signals, such as the fifth-order response measured in carbon disulfide by Tominaga *et al.*,[15] should vanish according to the harmonic theory[7] of higher-order Raman echo experiments. This theoretical consequence of the second integral term in eq 3 is due to the quadratic dependence of that term on the coordinates Q and the associated pulse delay(s): in multiple pulse probes where more than one delay τ is needed to describe the pulse sequence, the second integral term describes the response "echo".[7] Neither the coordinate identity of individual modes in Q nor the qualitative details of the modes (*e.g.*, damping) are in any way implicated in the presence or absence of this term in the response.

Other considerations also suggest that a DSE type orientational coordinate may not unilaterally account for the exponential tail of the OHD-RIKES transient in hydrogen-bonded liquids. With respect to orientational degrees of freedom in liquid water, it is unclear whether the large extended molecular clusters stay intact longer than the cluster rotation time since the hydrogen-bond lifetime has been suggested to be around 500 fs.[16] In addition, cascaded dipole−induced-dipole effects could lead to a depolarization rate, through dipolar hopping, faster than molecular rotation. Either of these effects would obscure rotational reorientation contributions (which for water have a 1/e time of ~8 ps[10]) to the experimental observable, although molecular reorientation would still contribute to homogeneous relaxation of the intermolecular modes in Q. In such a case, an analytical paradigm alternate to that of the classical DSE representation may be warranted. The Brownian oscillator representation of the OHD-RIKE response thus has interesting implications for analyses of dynamical mode coupling and structural relaxation in the condensed phase and constitutes a physically intuitive starting point for an exploration of the rates and paths of energy propagation from initially excited high-frequency, localized structural modes into lower-frequency, delocalized modes which may ultimately be observed macroscopically.

The existence of nonlinear coupling of the coordinates Q to the polarizability means that the line broadening details of the spectral density function cannot be recovered by direct Fourier transformation of the OHD-RIKE transient; instead, an analysis based on the more complicated response function of eq 3 is necessary. The response function of eq 3 invokes additional contributions to the third-order response and allows that the amplitude of the observed long time relaxations may partly result from nonlinear coupling of the polarizability to the nuclear coordinates Q and not only from the contribution of a noninteracting molecular orientation degree of freedom to a linear $R^{(3)}(\tau)$ (eq 6). In contrast to the linear (α_1^2) term, the quadratic (α_2^2) contribution to the response function $R^{(3)}(\tau)$ is biased to lower frequencies due to the presence of the hyperbolic cotangent thermal occupation function. The line shape functions J have a viscosity dependence similar to a DSE rotational reorientation through c_k^s (eq 11, *vide infra*) via the homogeneous dephasing constant γ in both the linear and quadratic contributions to $R^{(3)}(\tau)$, but γ appears to higher order in the α_2^2 term due to the quadratic dependence on J. Due to these distinctions in functional dependence, the α_2^2 term of $R^{(3)}(\tau)$ will be significantly more sensitive than the α_1^2 term to parameters that affect the dephasing rate, such as the (coordinate) moment of inertia, temperature, and mode coupling.

In this report, contributions of the quadratic coupling term (the α_2^2 term in eq 3) are used to exemplify the effects of a more general higher-order dependence of the medium polarizability on (harmonic) nuclear coordinates, such as the exponential coupling cited above. When the medium polarizability depends nonlinearly on intermolecular coordinates, the nonlinear response function $R^{(3)}(\tau)$ will contain information about the coupling between and broadening of specific spectral bands through the state variable dependence of the static (inhomogeneous) and dynamic (homogeneous) contributions to $C(\omega)$. This information can be recovered by fitting the experimentally

measured transients to a system of equations analogous to eqs 3−5 at each value of a varied state parameter. The specific functional form of the coupling in eq 2 (*e.g.*, polynomial, exponential, *etc.*) will affect the number and weighting of the terms in the nonlinear response function, but the qualitative trends will be similar for any nonlinear coupling.[7] Once the various contributions to $R^{(3)}(\tau)$ have been identified within a physical model, the $C(\omega)$ can be factored into homogeneous and inhomogeneous terms (*vide infra*). This procedure, which analyzes the (model-based) parametric dependence of a single-time correlation function through the third-order optical nonlinearity, is to be contrasted with higher-order nonlinear optical measurements of multiple-time correlation functions which can directly distinguish the unique time orderings of homogeneous and inhomogeneous modulations.[7,15]

We noted above that the linear α_1^2 term in the response $R^{(3)}(\tau)$ is incapable of discriminating homogeneous and inhomogeneous contributions and that a purely linear $R^{(3)}(\tau)$ is identical in the homogeneous and inhomogeneous limits. Physically, the linear term gives rise to optical phase interference between individual oscillators in the ensemble, and therefore its decay depends only on the total spectral distribution. However, the homogeneous and inhomogeneous contributions enter into the quadratic α_2^2 term of $R^{(3)}(\tau)$ differently. This can be explicitly seen in the homogeneous ($S(\omega_s) = \delta(\omega_s)$) and inhomogeneous ($J(\omega,\omega_s) = \delta(\omega-\omega_s)$) limits

$$R_{\mathrm{in}}^{(3)}(\tau) = \frac{2i\alpha_1^{\,2}}{\hbar}\int d\omega_s\, S(\omega_s)\sin\omega_s\tau + \frac{2i\alpha_2^{\,2}}{\hbar}\int d\omega_s\, S(\omega_s)\sin\omega_s\tau\cos\omega_s\tau\coth\frac{\beta\hbar\omega_s}{2} \quad (7)$$

and

$$R_{\mathrm{ho}}^{(3)}(\tau) = \frac{2i\alpha_1^{\,2}}{\hbar}\int d\omega\, J(\omega)\sin\omega\tau + \frac{2i\alpha_2^{\,2}}{\hbar}\int d\omega\, J(\omega)\sin\omega\tau\int d\omega'\, J(\omega')\cos\omega'\tau\coth\frac{\beta\hbar\omega'}{2} \quad (8)$$

where any distributions in the coupling strengths (η_s) and damping rates (γ_s) have been ignored, so that $S(\Gamma) = S(\omega_s)$ is the frequency distribution responsible for inhomogeneous dephasing. The second term containing two-quantum transitions results from time-ordered couplings within the ensemble of oscillators and frequencies generated through thermally excited bath fluctuations. The bath fluctuations are causally related to the homogeneous contribution in the spectral density of specific intermolecular degrees of freedom, and the quadratic dependence of the second term in eq 8 on $J(\omega)$ allows discrimination between homogeneous and inhomogeneous effects. This can be seen explicitly in Figure 1, which shows the linear and quadratic terms for $R^{(3)}(\tau)$ in the homogeneous and inhomogeneous limits of the spectral density $C(\omega)$. The parametrization of $C(\omega)$ (obtained by fitting the Fourier transform of the OHD-RIKES transient of H_2O with functions for J and S as discussed below) resulted in identical linear coupling dynamics (the α_1^2 terms of eqs 7 and 8) in the homogeneous and inhomogeneous limits, since the dependencies of the α_1^2 integral on the line shape functions are equivalent. In contrast, the quadratic α_2^2 term decays rapidly in the homogeneous limit with a time constant of approximately 85 fs, while the inhomogeneous limit shows nonexponential behavior with long-lived components >2 ps. These results, which are a consequence of the order of the

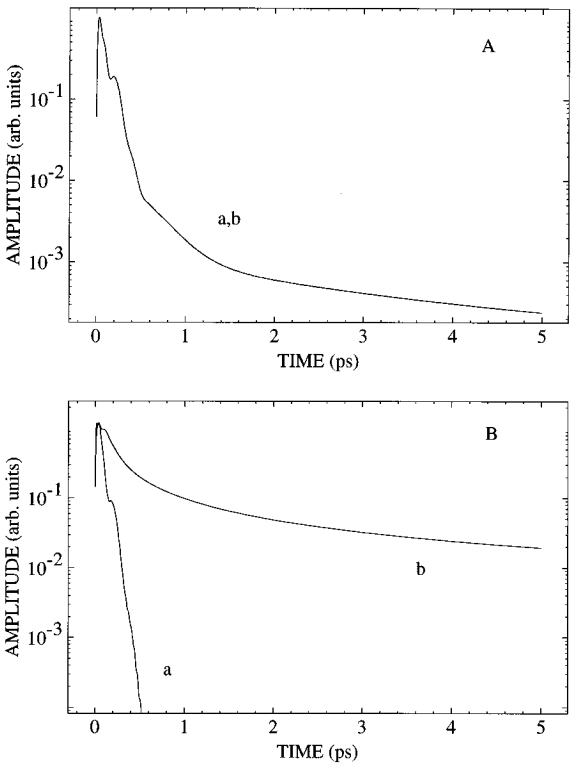

Figure 1. Homogeneous (a) and inhomogeneous (b) limits for the linear (A) and quadratic (B) coupling of the polarizability and nuclear coordinates of $R^{(3)}$. The linear term is identical in these two limits, while the quadratic term shows a fast decay of 85 fs for the homogeneous limit and nonexponential behavior with relaxations of >2 ps for the inhomogeneous limit.

nuclear degrees of freedom Q in the polarizability (eq 2) and not the parametrizations of S and J, illustrate the difficulty in the assignment of this component of the measured response and the need to assess the importance of the quadratic term through its state variable dependence.

These arguments indicate that, in practice, the homogeneous and inhomogeneous contributions to the line shape can be estimated through third-order measurements for the nonlinear coupling model. Since discrimination arises in the second (or higher)-order term(s), these measurements require that the homogeneous and inhomogeneous distributions are distinguishably altered as a state parameter is varied and that the amplitude of the nonlinear term (α_2^2) in the response functions (eqs 7 and 8) is above the experimental signal-to-noise ratio. In order to correlate simulations to experimental measurements, the functional dependencies of S and J on experimentally accessible parameters (*i.e.*, temperature, viscosity, molecular mass, *etc.*) are required. The form for $J(\omega;\Gamma)$ can be obtained assuming that each nuclear mode is coupled to a set of bath harmonic oscillators with coordinates x_k^s and momentum p_k^s.[17−19] The interaction between the system and the kth bath oscillator is assumed to be linear, with coupling strength c_k^s. The total Hamiltonian can be written as[7a]

$$H_{\mathrm{g}}(p,q) = \sum_s\left[\frac{p_s^{\,2}}{2m_s} + \frac{1}{2}m_s q_s^{\,2}\omega_s^{\,2} + \sum_{k\neq s}\left\{\frac{(p_k^s)^2}{2m_k^s} + \frac{m_k^s(\omega_k^s)^2}{2}\left(x_k^s - \frac{c_k^s q_s}{m_k^s(\omega_k^s)^2}\right)^2\right\}\right] \quad (9)$$

By tracing over the nuclear and bath coordinates[20]

$$J^s(\omega) = \frac{\omega\eta_s\gamma_s(\omega)}{2\pi((\omega_s^2 - \omega^2)^2 + \omega^2\gamma_s^2(\omega))} \tag{10}$$

where

$$\gamma_s(\omega) = \sum_k \frac{(c_k^s)^2}{2m_k^s(\omega_k^s)^2}\delta(\omega - \omega_k^s) \tag{11}$$

Assuming a frequency-independent damping $\gamma_s(\omega) = \gamma_s$

$$\sum_s J^s(\omega) \rightarrow J(\omega;\Gamma) = \sum_s \frac{\omega\eta_s\gamma_s}{2\pi((\omega_s^2 - \omega^2)^2 + \omega^2\gamma_s^2)} \tag{12}$$

where the sum over s signifies that in general each physical mode of the system can have a different effective homogeneous width and coupling strength. Here γ_s is related, in the liquid phase, to a viscosity-dependent term, c_k^s, and a molecular mass-dependent term, m_k^s, analogous to the classical Langevin equation.[21]

Previous work has shown that only higher-order Raman experiments can directly separate homogeneous and inhomogeneous components to the spectral density.[7,20] The term "directly" in this context means "in a single experiment and without any further knowledge of the line shape functional forms and/or their dependencies on physically accessible parameters". The method presented here is not inconsistent with that premise, since the homogeneous and inhomogeneous contributions can only be extracted if a physical model provides the functional dependencies of the respective line shape contributions. Thus, there is basically a hierarchy of assumptions which must be made to extract the homogeneous and inhomogeneous contributions. While higher-order (fifth, seventh, ···) Raman experiments require no assumptions regarding the functional forms of the inhomogeneous and/or homogeneous distributions,[7,20] there are many experimental difficulties that must be overcome in order to acquire data with sufficient signal-to-noise for an unambiguous interpretation. Conversely, a series of third-order Raman experiments in which temperature (viscosity), isotopic composition, or number density are varied can provide high-quality, high-signal-to-noise data for detailed analyses of the above-mentioned "physically reasonable" assumptions regarding the dependence of the homogeneous and inhomogeneous line shape on these parameters. These conditions are to be contrasted with a third-order measurement at a single set of state parameters, which requires that the exact functional forms of both homogeneous and inhomogeneous distributions be known through well-founded theoretical arguments, as in gas phase experimental studies.

Experimental Results and Numerical Calculations

The laser source for these experimental studies was a Ti:sapphire laser synchronously pumped by 5 W from a mode-locked and frequency-doubled Nd:YAG laser. The Ti:sapphire laser produces 30−40 fs (fwhm) pulses at 76 MHz and average powers up to 1.0 W.[22] The experimental method for the heterodyne-detected Raman-induced Kerr effect studies is identical to that described previously.[6,9] The pure out-of-phase (OP) heterodyne responses have been constructed from data scans collected with positively and negatively sensed local oscillators,[6,9] which eliminates homodyne contamination of the heterodyne signal. The temperature dependence of the low-frequency Raman-active modes in water was investigated by using temperature-controlled flowing and static cells. The liquid temperature was monitored and stable to ±0.2 °C or better. Figure 2 shows representative pure OP OHD-RIKE responses for temperatures of 2.6, 24.0, 53.5, and 92.0 °C. It can be seen that the long-lived exponential relaxation becomes increasingly shorter with increasing temperature (decreasing viscosity). As can be seen from eq 9, contributions to $R^{(3)}(\tau)$ would also be expected to exhibit a dependence on the molecular mass or moment of inertia. Experimental results on D_2O have been found to be consistent with this theoretical description.[23]

Figure 3 displays the Fourier transforms of the OHD-RIKES transients shown in Figure 2 at 2.6, 24, and 53.5 °C and calculated according to our previous prescription.[6,9] The spectral density derived from this analysis presumes the linear coupling hypothesis which results in eq 6. This spectral density, which we take as our default $C(\omega)$ (eq 1), changes with temperature as follows: the modes centered near 60 and 170 cm^{-1} shift to lower frequency, and the 170 cm^{-1} mode appears to broaden and decrease in amplitude, while the librational modes between 350 and 600 cm^{-1} increase in amplitude with increasing temperature. There is an inherent uncertainty in the behavior of the spectral amplitudes in the 350−600 cm^{-1} range due to uncertainty in the precise position of the time origin of the OHD-RIKES experiment which we have noted previously.[6] The changes in the band shape at frequencies <300 cm^{-1} are substantially independent of this effect. The evolution of the spectral density with temperature contains specific information about the structure and dynamical properties of the liquid, which we want to extract unencumbered by the possibility of analytical artifacts. The analytical procedures employed by the Brownian oscillator analysis developed herein extract the temperature dependence of the medium response in the time domain, prior to the discrete Fourier-transform manipulations which are sensitive to the above-mentioned details regarding the precise experimental time origin. In this regard, the results of the Brownian oscillator analysis serve to validate qualitative conclusions emerging from the direct Fourier-transform analysis represented in Figure 3.

The calculated temperature dependence of the terms in $R^{(3)}(\tau)$ within the quadratic coupling limit of the Brownian oscillator model (eqs 3−5, 11, 12) are shown in Figure 4. The precise functional form of the inhomogeneous distribution used in these calculations is not critical, as other functional forms give similar results. In this instance the inhomogeneous distribution was assumed to be of the form

$$S(\omega) = \sum_m \frac{\omega^2 A_m C_m}{2\pi((\omega^2 - B_m^2)^2 + \omega^2 C_m^2)} \tag{13}$$

where the index m specifies physically different modes which contribute to the spectral distribution (*i.e.*, librations, translations). The inhomogeneous parameters extracted from the fit are $A_{1\cdots5}$ (cm^{-1}) = (1.4, 2.6, 6.7, 5.8, 10.0), $B_{1\cdots5}$ (cm^{-1}) = (70, 200, 420, 570, 720), and $C_{1\cdots5}$ (cm^{-1}) = (140, 140, 240, 240, 240) where A is related to the relative amplitudes of each mode, B the center frequencies, and C to the width of the inhomogeneous distribution around each mode. The number of terms and their center frequencies were chosen to be consistent with the results of previous spontaneous Raman scattering measurements.[24] The librational bands centered at 420, 570, and 720 cm^{-1} could be fit with a single broad band to reduce the number of terms in the fitted spectral density, but such a computational simplification would not affect the results due to the presence or absence of the nonlinear coupling.

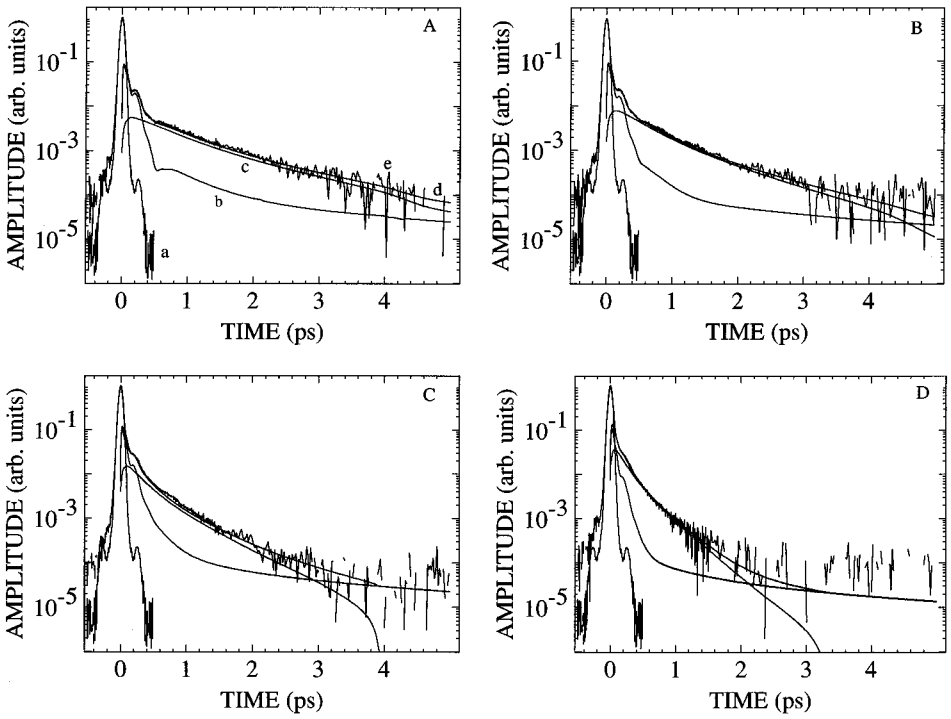

Figure 2. Temperature-dependent fits to time domain responses at (A) 2.6, (B) 24.0, (C) 51.9, and (D) 92.0 °C utilizing electronic hyperpolarizability contribution and calculated linear and quadratic nuclear terms. These terms are identified by the relative peak amplitudes: electronic (a) > linear (b) quadratic (c). Curves (d) are the calculated fits to the experimental data (e). The homogeneous line width is 16, 29, 52, and 83 cm^{-1}, respectively. Note that these responses are still convolved with the finite laser pulse width.

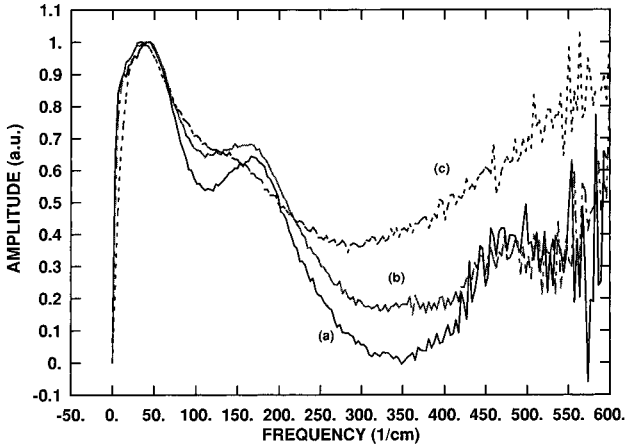

Figure 3. Temperature dependence of the spectral densities $C(\omega)$ of the OHD-RIKE wave forms shown in Figure 2 and obtained by discrete Fourier-transform analysis premised on the linear coupling hypothesis of eq 6: (a) corresponds to 2.6 °C, (b) to 24 °C, and (c) to 92 °C.

In these fits three assumptions are made regarding the parametrization of the spectral density. Two of these pertain to the inhomogeneous distribution. The first is that the center frequencies and amplitudes of the inhomogeneous distribution are slowly varying relative to changes in the homogeneous damping that result from viscosity variations within the temperature range studied. This assumption is supported by MD simulations of hydrogen-bonded water clusters which indicate that the cluster size, and hence the local environment of molecules in a cluster, is not a strong function of temperature.[25] Second, there exists a low-frequency cutoff in the inhomogeneous distribution which depends on the time scale of bath fluctuations that redistribute molecules into new clusters. Physically, this cutoff simply recognizes the practical restriction of "slow" line broadening processes to time scales longer than the (underdamped) oscillator period.[26] Computationally, this cutoff frequency is given by the product of a temperature-independent coefficient (which varies with the functional form chosen for the inhomogeneous distribution) and the effective homogeneous damping. Lastly, to simplify this demonstration of the multimode analysis, the number of parameters in the fitted spectral density is restricted by our assumption of a single homogeneous damping parameter γ for all of the modes.

The linear term (panel A) shows a qualitative temperature dependence for the high-frequency oscillations that is consistent with the experimental results for time delays <1 ps: as the temperature is increased, the oscillations become less distinct. This part of $R^{(3)}(\tau)$, however, does not show the observed temperature dependence of the longest-lived relaxations. The linear term can fitted to the measured response to account for the dynamics at a single temperature, but the time constant of the exponential tail in the calculated response decreases incommensurably with that of the measured response as the temperature is varied. The temperature scaling of the linear term is due to increased broadening of the homogeneous line shape. This broadening arises from the coupling term c_k^s in eqs 9 and 11, which in these calculations is related to the inverse of the temperature-dependent shear viscosity.[27] As the temperature rises, the viscosity decreases and the damping rate (and homogeneous line width parameter) γ increases. The quadratic term (panel B), on the other hand, shows behavior that is consistent with the measured temperature dependence of the exponential tail. The enhanced temperature sensitivity of the quadratic term derives from both the higher-order dependence on the homogeneous damping γ and the hyperbolic cotangent describing the thermal occupation of the modes. The exact position of the peak depends on the homogeneous damping rate in the line shape function which ranges from 150 fs at 4.5 °C to 80 fs at 92 °C (see Figure 4C). This is similar to the overdamped oscillator dynamics assumed in the tail-matching procedure of McMorrow and Lotshaw.[8] In the present case, this contribution results from the nonlinear coupling of the

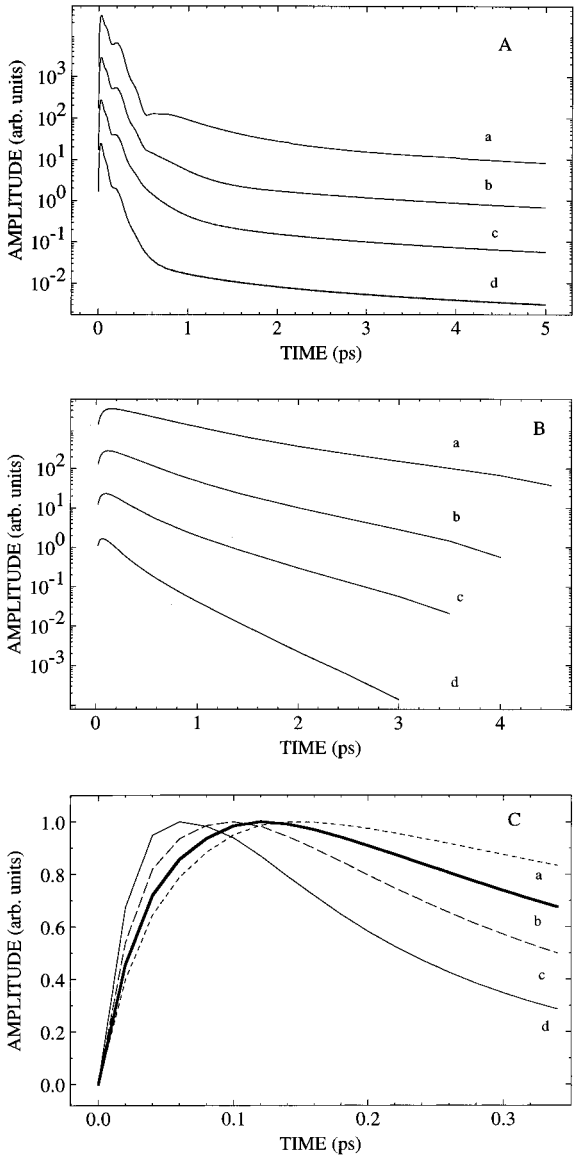

Figure 4. Calculated temperature dependence of the nuclear response function with mixed line broadening within the multimode Brownian oscillator model for nonlinear coupling of nuclear coordinates and polarizability at (a) 2.6, (b) 24.0, (c) 52.0, and (d) 92.0 °C: (A) linear term and (B) quadratic term; (C) dependence of the rise time on the homogeneous contribution to the distribution which changes as a function of temperature. The curves are offset for clarity.

polarizability and nuclear coordinates and not from a noninteracting reorientational mode. This component, however, shows behavior analogous to such a reorientation coordinate; namely, the molecular mass- and viscosity (temperature)-dependent studies show the decay becomes longer with increased molecular moment and shorter with lowered viscosity.

The global fit to the temperature-dependent data was obtained within the Brownian oscillator model using the linear and quadratic terms of eq 3. It should be noted that these calculations still retain the finite spectral bandwidth of the laser since the comparisons are made to experimental OHD-RIKE responses without deconvolution. Increasing the homogeneous contribution to the line shape of each mode at low temperatures will cause the response to evolve more rapidly with temperature, thereby allowing the determination of homogeneous part to the spectral distribution. The correlations between the calculated best fit and experimental data are shown in Figure 2. The extracted homogeneous line widths (γ) are 16, 29, 52, and 83 cm^{-1} at 2.6, 24.0, 51.9, and 92.0 °C, respectively. In addition

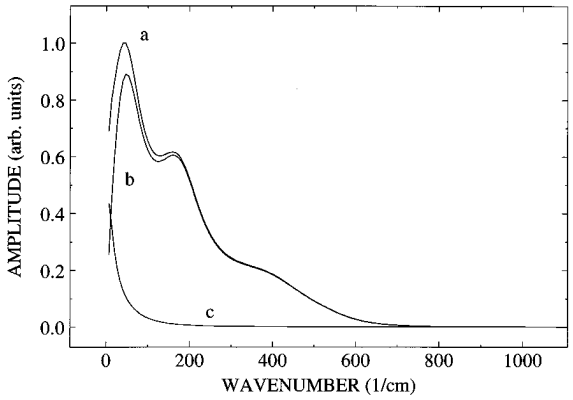

Figure 5. Spectral density functions for 2.6 °C response: total spectral density (a), linear coupling term (b), and quadratic coupling term (c). Note that these spectral densities are still convolved with the finite laser spectral bandwidth.

to the nuclear response, an electronic contribution will also be present in the experimental OHD-RIKE response. Within the Born−Oppenheimer approximation, and for off-resonance excitations, the nuclear and electronic contributions will be separable with the electronic contribution following the autocorrelation.[2,8] The fit, consisting of the electronic hyperpolarizability and the linear and quadratic nuclear contributions, is also shown in Figure 2. It can be seen that the calculated responses are in good qualitative agreement with the experimental measurements. The corresponding frequency domain representation is shown for the 2.6 °C fit in Figure 5. (The curves presented in Figure 5 cannot be directly compared to the 2.6 °C spectral density shown in Figure 3, since the curves in Figure 3 have been deconvoluted from the spectral density function of the exciting laser pulse. The deconvolution has two effects: the amplitude and the amplitude noise increase with increasing frequency, the former due to the decreasing amplitude in the wings of the (finite) laser spectrum and the latter due to the quotient of two small numbers in the deconvolution calculation at high frequencies (>2 times the fwhm laser bandwidth).[6,9]) It can be seen that the quadratic term affects the low-frequency portion of the spectrum most dramatically due to the presence of the hyperbolic cotangent thermal occupation term. This behavior, as well as the actual spectral density of the quadratic term, is also heuristically consistent with the simpler DSE interpretation of a noninteracting, molecular reorientation mode due to isolated molecules reorienting within a viscous dielectric continuum, as was noted above. However, the mechanism of the observable is now open to a more appropriately convoluted interpretation in which the dynamics of the various higher-frequency intramolecular and intermolecular modes of the medium explicitly couple and thereby contribute to the low-frequency, "diffusive" response component. Such considerations are especially relevant to the coupling between the underdamped librational motions which exhibit zero root-mean-square (rms) displacement and "diffusive" (DSE) reorientation which exhibits finite rms displacement in the same molecular orientational coordinate.

Concluding Remarks

A linear dependence of the polarizability on harmonic nuclear degrees of freedom in molecular liquids is inconsistent with experimental observations of higher-order Raman responses in the liquid phase and the measured temperature dependence of the third-order nonlinear response function $R^{(3)}(\tau)$ for the hydrogen-bonding liquid water. Inclusion of a quadratic dependence of the medium polarizability on the nuclear degrees

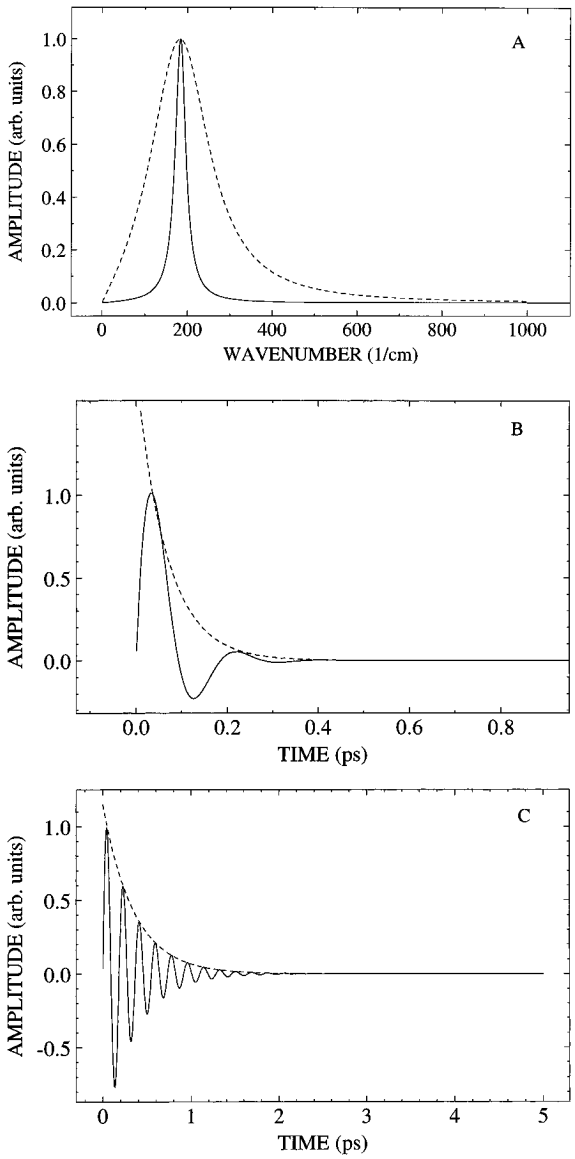

Figure 6. Homogeneous and inhomogeneous contributions for one mode within the Brownian oscillator model. (A) This figure shows the line width for the 200 cm^{-1} mode using the extracted homogeneous line width of 30 cm^{-1} (solid) as well as the experimentally obtained spectral distribution (dashed line). It can be see that the distribution has significant contributions arising from inhomogeneous contributions. (B, C) Time domain analog for these contributions. The envelope decay for the inhomogeneous distribution is 65 fs while that of the homogeneous contribution is 350 fs.

of freedom results in a reasonable account of the temperature dependence of the OHD-RIKE experimental results for water. This nonlinear coupling model addresses both the temperature dependence of the high-frequency oscillations and long-time relaxations, thereby eliminating potential inconsistencies in the extraction of the vibrational spectral density distribution from the OHD-RIKE temporal wave form. In addition, the multimode Brownian oscillator model (with nonlinear coupling) indicates that temperature- and isotope-dependent third-order nonlinear optical studies enable an estimate of the homogeneous contribution to the spectral density function. These studies indicate that the liquid water system is highly inhomogeneous. For example, the extracted homogeneous line width at 24.0 °C is 29 cm^{-1} compared to an inhomogeneous width of 140 cm^{-1} for the low-frequency Raman-active modes. These relative bandwidths can be seen explicitly in Figure 6A, which illustrates the total distribution for the 200 cm^{-1} mode and the homogeneous contribution for one mode within the inhomogeneous distribution. The Fourier-transform dynamics of these terms is shown in Figure 6B,C, respectively.

We have observed that the precise functional forms of the homogeneous and inhomogeneous line shape functions do not materially alter the qualitative effects of nonlinear coupling on the dynamics or parameter scaling of the nonlinear response function $R^{(3)}(\tau)$, or the parameters extracted by this analysis. It is the coordinate coupling, not the number of terms in the line shape functions, that qualitatively affects the state-parametric behavior of the nonlinear response $R^{(3)}(\tau)$. Additionally, it is important to understand that the qualitative distinctions between the linear and nonlinear terms of $R^{(3)}(\tau)$, as well as the effects of the line broadening mechanisms on the dynamics of the nonlinear term, do not depend upon a highly multimode spectral density like that of water. [Note, however, that even highly symmetric "simple" liquids like CS_2 exhibit an intermolecular spectral density composed of at least two modal contributions.[26,28]]

The parameters deduced from our analysis can be used to calculate both the relative amplitude and dynamics of higher-order correlation responses, which can directly determine inhomogeneous contributions to the line shape. This application of the OHD-RIKE spectral density has been described previously[29] and can be used to bracket the range of some experimental parameters required for the higher-order Raman probe. For example, the 29 and 140 cm^{-1} homogeneous and inhomogeneous line width contributions to the 200 cm^{-1} mode correspond to 350 and 65 fs 1/e times, respectively, and imply that sub-50 fs pulse widths are required for fifth-order measurements on this liquid. In addition, by assuming a specific coupling form, the relative amplitudes for third- and higher-order experiments can be determined. For the coupling specified by eq 2, the coefficients for the linear and quadratic terms are given by $2\alpha_1^2/\hbar$ and $2\alpha_2^2/\hbar$, respectively, and a ratio of 50:1 is obtained for the relative amplitudes from the experimental fits. When combined with the signal amplitude of the third-order response under the experimental excitation conditions, this ratio allows an estimation of the fifth-order signal amplitude in the quadratic coupling limit. From these conditions it is found that an excitation intensity of 30 GW/cm^2 will produce an equivalent signal amplitude in the fifth-order response as 6 GW/cm^2 did in the third-order OHD-RIKES measurement. This scaling implies that a $\chi^{(5)}$ signal should be observable and separable from the $\chi^{(3)}$ signal at excitation levels achievable even with unamplified, cavity-dumped Ti:sapphire lasers.

The intent of our analysis is not to unilaterally dismiss the DSE representation, but to propose an alternate *additional* mechanism (and interpretation) that can account for *anomalous* parametric behavior of a "DSE-like" relaxation. The response function $R^{(3)}(\tau)$ given by eq 3 contains *both* the linear and nonlinear contributions: the linear contribution of any orientational coordinate has not been discarded. The lack of convergence between the measured 1/e times of the "exponential part" of the OHD-RIKES and NMR transient cannot be attributed to the distinction of isomolecular and collective relaxations.[30] Such distinctions commonly result in deviations on the order of unity in the measured response times,[30] as opposed to the observed deviation on the order of 10 in the case of water. This magnitude of deviation is heuristically consistent with the effective broadening of the response (non-Lorentzian) spectral density due to contributions of the higher-frequency modes in the "wings" of the nonlinear term (curve c, Figure 5). By explicit inclusion of couplings which allow for energy migration from higher-frequency structural modes to low-frequency modes which account for structural relaxation, the Brownian oscillator model is capable of accounting for the

coupling of coordinates whose motions exhibit zero net displacement (underdamped oscillators) and coordinates that exhibit finite net displacement and hence structural relaxation.

Further theoretical and experimental work is underway to explore the physical nature of the mode damping and coupling and to determine whether terms similar to those obtained due to the nonlinear coupling of harmonic nuclear coordinates and the polarizability can arise in a representation using anharmonic oscillators.

Acknowledgment. Support of this research was provided in part by the NSF Science and Technology Center on Photoinduced Charge Transfer (Grant CHE 9120001) and the General Electric Co.

References and Notes

(1) Yan, Y.-X.; Gamble, Jr., E. B.; Nelson, K. A. *J. Chem. Phys.* **1985**, *83*, 5391.

(2) McMorrow, D.; Lotshaw, W. T.; Kenny-Wallace, G. A. *IEEE Quantum Electron.* **1988**, *24*, 443.

(3) Scherer, N. F.; Ziegler, D.; Fleming, G. R. *J. Chem. Phys.* **1992**, *96*, 5544.

(4) Barker, C. E.; Trebino, R.; Kostenbauder, A. G.; Siegmann, A. E. *J. Chem. Phys.* **1990**, *92*, 4740.

(5) Hatori, T.; Kobayashi, T. *J. Chem. Phys.* **1991**, *94*, 3332.

(6) Palese, S.; Schilling, L.; Miller, R. J. D.; Staver, R.; Lotshaw, W. T. *J. Phys. Chem.* **1994**, *99*, 6308.

(7) (a) Tanimura, Y.; Mukamel, S. *J. Chem. Phys.* **1993**, *99*, 9496. (b) Khidekel, V.; Mukamel, S. *Chem. Phys. Lett.* **1995**, *240*, 304.

(8) (a) Lotshaw, W. T.; McMorrow, D.; Kenney-Wallace, G. A. *Proc. SPIE* **1988**, *981*, 20. (b) McMorrow, D.; Lotshaw, W. T. *Chem. Phys. Lett.* **1990**, *174*, 85.

(9) Lotshaw, W. T.; McMorrow, D.; Thantu, N.; Melinger, J. S. *J. Raman Spectrosc.* **1995**, *26*, 571.

(10) Madden, P. A.; Cox, T. I. *Mol. Phys.* **1981**, *43*, 287.

(11) Barthel, J.; Bachhuber, K.; Buchner, R.; Hetzenauer, H. *Chem. Phys. Lett.* **1990**, *165*, 369.

(12) We have been unable, after repeated measurements on H_2O and D_2O over a wide range of temperatures, to observe a relaxation component with the 1/e time of 1.2 ps reported by Chang and Castner (Chang, Y. J.; Castner, E. W., Jr. *J. Chem. Phys.* **1993**, *99*, 7289) using an unamplified Ti:sapphire laser for excitation at 800 nm. We have observed a small-amplitude 1.8 ps relaxation when an amplified dye laser at 625 nm was used (ref 6).

(13) Ohmine, I.; Tanaka, H. *J. Chem. Phys.* **1990**, *93*, 8138.

(14) Cho, M.; Du, M.; Scherer, N.; Fleming, G. R. *J. Chem. Phys.* **1993**, *99*, 2410.

(15) Tominaga, K.; Keogh, G. P.; Naitoh, K.; Yoshihara, K. *J. Raman Spectrosc.* **1995**, *26*, 495.

(16) Montrose, C. J.; Bucaro, J. A.; Marshall-Coakley, J.; Litovitz, T. A. *J. Chem. Phys.* **1974**, *60*, 5025.

(17) Caldiera, A. O.; Leggett, A. J. *Physica A* **1983**, *121*, 587.

(18) Grabert, N.; Schramm, P.; Ingold, G. L. *Phys. Rep.* **1988**, *168*, 115.

(19) Silbey, R.; Harris, R. A. *J. Phys. Chem.* **1989**, *93*, 7062.

(20) Tanimura, Y.; Mukamel, S. *Phys. Rev. E* **1993**, *47*, 118.

(21) Pathria, R. K. In *Statistical Mechanics*; Pergamon Press Elmsford: New York, 1972; p 456.

(22) Staver, P. R.; Lotshaw, W. T. Submitted to *Opt. Lett.*

(23) Palese, S.; Mukamel, S.; Miller, R. J. D.; Lotshaw, W. T. To be submitted to *J. Phys. Chem.*

(24) Walrafen, G. E. *J. Phys. Chem.* **1990**, *94*, 2237.

(25) Bosma, W. B.; Fried, L. E.; Mukamel, S. *J. Chem. Phys.* **1993**, *98*, 4413.

(26) McMorrow, D.; Lotshaw, W. T. *Chem. Phys. Lett.* **1991**, *178*, 69.

(27) *CRC Handbook of Chemistry and Physics*, 74th ed.; CRC Press: Boca Raton, FL, 1994; Chapters 6, 10.

(28) McMorrow, D.; Thantu, N.; Melinger, J. S.; Kim, S. K.; Lotshaw, W. T. *J. Phys. Chem.* **1996**, *100*, 10389.

(29) Palese, S.; Bountempo, J.; Schilling, L.; Miller, R. J. D.; Tanimura, Y.; Mukamel, S.; Lotshaw, W. T. *J. Phys. Chem.* **1994**, *98*, 12466.

(30) Berne, B. J.; Pecora, R. *Dynamic Light Scattering*; John Wiley and Sons: New York, 1976; Chapter 12.3, p 321.

JP960266L